High-Density Integration of High-Frequency High-Current Point-of-Load (POL) Modules With Planar Inductors

Wenli Zhang, Yipeng Su, *Student Member, IEEE*, Mingkai Mu, David J. Gilham, Qiang Li, *Member, IEEE*, and Fred C. Lee, *Life Fellow, IEEE*

***Abstract*—Planar inductors made by mixed laminates of low-temperature sintered Ni-Cu-Zn ferrite tapes and metal-flake composite materials are used for high-density integration of point-of-load (POL) modules. Incremental permeability and core loss density were characterized on toroidal samples under high dc bias to demonstrate that both materials are suitable for application in high-frequency high-current POL converters. In order to realize a high power density POL module, a multilayer ferrite inductor laminated with alternating layers of ESL 40010 and ESL 40012 in a 1:1 ratio has been fabricated and integrated with the active layer. Meanwhile, standard printed circuit board (PCB) processing has been adopted for the POL integration with a PCB-embedded inductor using NEC-TOKIN's metal-flake composite materials. These developed 3-D integration approaches can be used to reduce the footprint and increase the power density for POL converters. It has been demonstrated that the power efficiency of both POL modules with integrated planar inductors can achieve above 87% at an operating frequency of 2 MHz and an output current of 15 A. Additionally, no obvious efficiency degradation was observed on the integrated POL modules after a certain number of thermal cycling from −40 °C to +150 °C.**

***Index Terms*—High-density integration, metal-flake composite, multilayer ferrite, planar inductor, point-of-load (POL) module.**

I. Introduction

HIGH power density point-of-load (POL) converters are highly desired to fulfill the requirements of miniaturization for the thriving portable electronic device market. Increasing switching frequency (>1 MHz) to reduce the size and weight of passives is a common route to increase the power density for POL converters. The emerging next-generation semiconductor power devices, such as gallium nitride (GaN-on-Si) transistors, offer potential benefits in various power conversion applications. This technology enables a high switching frequency of up to several megahertz. Another path to high power density is through the integration of capacitors and inductors. In today's POL modules, the magnetic components consume the largest footprint and are the most limiting factor for high-density integration. With the increasing demand to reduce the size of power inductors, magnetic core materials with low energy loss and high permeability under high dc bias as well as high operating frequency are urgently needed. Moreover, such magnetic materials have to be compatible with conventional or newly developed integration techniques for power electronics applications [1], [2].

The high-density integration techniques can be classified into two categories: wafer-level integration and package-level integration. Tremendous effort has been put into integrating the inductor and transformer on or in the silicon die at the wafer level. Magnetic components can be built either on top of or beside the active circuitry in the same die. These integration processes are compatible with established silicon processing techniques [3], [4]. However, the on-chip wafer-level integration is only suitable for low current (<5 A) applications using the currently available materials and technologies. Integrating passives with power devices and active circuitry at the package-level may be feasible for high current (>10 A) applications [2]. In this copackaged configuration, magnetic passives and all other components can be assembled either side-by-side or by stacking on each other in the same module.

A series of studies have been performed on the realization of the high-density integration of high-frequency high-current POL modules at the Center for Power Electronics Systems (CPES). Low-profile planar low temperature co-fired ceramic (LTCC)-based inductor substrates with lateral flux patterns were designed and evaluated for multimegahertz 3-D integrated POL modules with GaN devices. The core thickness and loss of the inductor were the main considerations in the design process. The impacts of different operation frequencies on the design of the LTCC inductor substrate were also studied [5], [6]. The designed planar inductor was subsequently used to fabricate integrated POL modules. The analysis on parasitic inductances and electrical layout for 3-D integrated POL modules reported that a size reduction of the high-frequency power loop could offer significant performance improvements and provide a smaller package size for the assembled module [7], [8]. Recently, our attempt of embedding a low-profile metal-flake inductor inside of the printed circuit board (PCB) substrate was also introduced [9].

This work provides detailed information regarding the development of new fabrication techniques using two different

Manuscript received October 31, 2013; revised March 7, 2014; accepted April 19, 2014. Date of publication April 29, 2014; date of current version October 15, 2014. This work was supported in part by the U.S. Department of Energy, ARPA-E project "Power Supplies on a Chip (PSOC)" under Grant DE-AR00000106. Recommended for publication by Associate Editor C. R. Sullivan.

The authors are with the Center for Power Electronics Systems, Bradley Department of Electrical and Computer Engineering, Virginia Polytechnic Institute and State University, Blacksburg, VA 24061 USA (e-mail: wzhang11@vt.edu; yipengsu@vt.edu; mmk@vt.edu; dgilham@vt.edu; lqvt@vt.edu; fclee@vt.edu).

Color versions of one or more of the figures in this paper are available online at http://ieeexplore.ieee.org.

Digital Object Identifier 10.1109/TPEL.2014.2320857

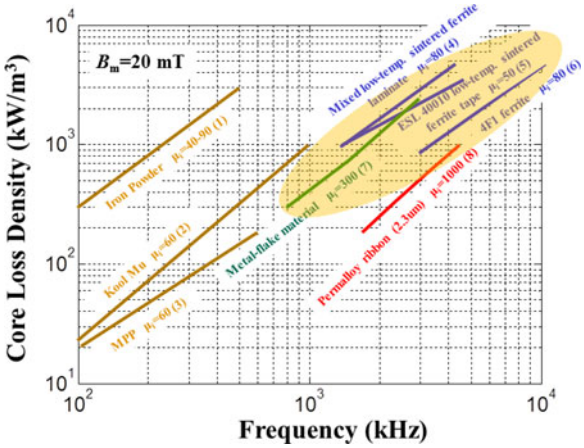

Fig. 1. Core loss density comparison of various magnetic materials under different frequencies. (1) Iron powder cores purchased from Ferroxcube. (2) Kool Mu cores purchased from magnetics. (3) MPP cores purchased from magnetics. (4) Mixed low-temperature sintered ferrite laminates developed by CPES. (5) ESL 40010 low-temperature sintered ferrite tapes purchased from ElectroScience. (6) 4F1 ferrite cores purchased from Ferroxcube. (7) Metal-flake composite materials obtained from NEC-TOKIN (in development). (8) Permalloy ribbon materials obtained from magnetics (in development). Please note that the curves (1), (2), (3), and (6) were replotted according to the manufacturers' datasheets.

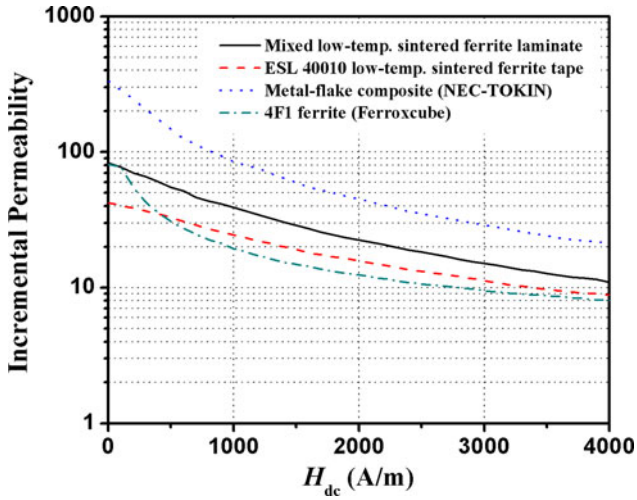

Fig. 2. Variation of incremental permeability measured at 1.5 MHz under dc bias for selected magnetic materials. Measurement temperature was set up at 100 °C.

magnetic materials for the integration of high-frequency high-current POL converters. Mixed low-temperature sintered ferrite laminates and metal-flake composite materials were chosen for the fabrication of planar inductors and further high-density integration of POL modules based on a comparison of core loss density and permeability with other candidate magnetic materials. The first POL module with a multilayer ferrite inductor substrate was fabricated using modified LTCC processing and hybrid integration techniques. The second module with a PCB-embedded metal-flake inductor was prepared using PCB processing techniques. The electrical performance and thermal reliability were then tested on both integrated high power density POL prototype modules. It is demonstrated that both selected magnetic materials and associated integration techniques are desired for integration of high-frequency high-current POL modules. The PCB-embedded inductor module may have a cost advantage due to the easy integration process and the feasibility of mass production.

II. Characterization of Magnetic Materials

The core loss density of a variety of magnetic materials was measured using a new high-frequency magnetic characterization tool introduced in [10] and [11]. The incremental permeability and core loss density under a dc bias of up to 4000 A/m were evaluated using the same experimental setup by applying an additional winding and dc current to the test samples [12].

Fig. 1 compares core loss density P_v of eight candidate magnetic materials in a frequency range from 100 kHz to 10 MHz. Core loss measurements were performed on toroidal samples at a flux density $B_{\rm m}$ of 20 mT and a temperature of 100 °C (Please note that the curves (1), (2), (3), and (6) shown in Fig. 1 were replotted based on the manufacturers' datasheets). The P_v of commercialized iron powder and Kool Mu cores increases to 1000 kW/m^3 at 250 kHz and 1 MHz, respectively. These two magnetic materials are not suitable for high-frequency (>1 MHz) applications. The MPP cores exhibit a lower P_v than the iron powder and Kool Mu cores in the same frequency range. However, the higher cost of MPP cores limits its widespread application in consumer products. Although the permalloy ribbon developed by magnetics exhibits high permeability and low P_v in the 1–5 MHz range, the small thickness (2.3 μm) and sensitivity to mechanical stress of this material limit its capability for inductor machining and POL module integration. The high-temperature sintered Ni-Zn ferrite (e.g., 4F1 from Ferroxcube) and low-temperature sintered Ni-Cu-Zn ferrite (e.g., ESL 40010 from ElectroScience) are commonly used for high-frequency applications because of their relatively low core loss density. A mixed low-temperature sintered Ni-Cu-Zn multilayer ferrite developed by CPES also shows acceptable P_v [13]. The P_v of NEC-TOKIN's novel metal-flake composite material is lower than that of low-temperature sintered Ni-Cu-Zn ferrites below 2–3 MHz, while it becomes higher beyond that frequency range.

In the designed high-frequency POL converters, high dc current is constantly applied to bias the inductors. It is, thus, important to consider the influence of dc bias on the magnetic properties of core materials exposed in high excitation levels. Considering the P_v at 1–5 MHz range, four magnetic materials, shown in the shaded area in Fig. 1, were selected for further investigation of the impact of superimposed dc bias on their magnetic properties, i.e., incremental permeability and core loss density.

The incremental permeability with applied dc bias of these four selected materials were measured at frequency f of 1.5 MHz and compared with each other, as shown in Fig. 2. The incremental permeability continuously decreases to only 7%–15% of its initial value as the superimposed dc bias $H_{\rm dc}$ increases from zero to 4000 A/m for all testing materials. It

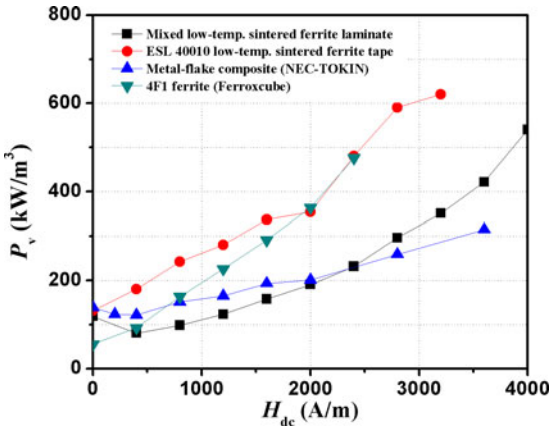

Fig. 3. Comparison of core loss density under dc bias for selected samples measured at $f = 1.5$ MHz, $B_{\rm m} = 10$ mT, and T = 100 °C.

is demonstrated that the NEC-TOKIN's metal-flake composite materials have the highest permeability among all examined samples throughout the whole $H_{\rm dc}$ range, which is highly desired for the high current POL application. The mixed low-temperature sintered ferrite laminates exhibit lower incremental permeability than the NEC-TOKIN's materials, but higher than the commercial ESL 40010 and 4F1 ferrites.

The changes in core loss density measured with a value of f of 1.5 MHz and a $B_{\rm m}$ of 10 mT with a superimposed dc bias for the chosen samples are illustrated in Fig. 3. The P_v for the commercial ESL 40010 and 4F1 ferrites continuously increases as $H_{\rm dc}$ increases, and the latter shows a relatively low P_v until the $H_{\rm dc}$ reaches 2400 A/m. The P_v measured on the mixed ferrite laminates and NEC-TOKIN's metal-flake composite materials initially decreases at 400 A/m and then increases; however, these two materials have a lower P_v at $H_{\rm dc}$ above 800 A/m when compared with the other two materials. The NEC-TOKIN's materials exhibit the lowest P_v when the superimposed $H_{\rm dc}$ is higher than 2400 A/m.

The designed planar inductors are expected to work at a high $H_{\rm dc}$ level of up to 4000 A/m during the normal operation of the integrated POL module. Therefore, considering the higher incremental permeability and lower core loss density, especially at that dc bias level, the mixed ferrite laminates developed by CPES and the metal-flake composite materials invented by NEC-TOKIN were chosen for the design and fabrication of planar inductors leading to high-density integrated POL modules.

III. Fabrication of Integrated POL Modules With LICC-Based Ferrite Laminates

As a well-established electronic packaging technology for the past three decades, LTCC materials and processing provide high-density electrical interconnects and hermetic packaging for integrated circuits. From the beginning of this century, LTCC processing techniques have been demonstrated to be an effective approach for the fabrication of low-profile power inductors and transformers using low-temperature sintered ferrite tapes [14]–[16]. LTCC-based ferrites are normally produced in tape format by tape-casting a slurry on polymeric carrier substrates in varying thickness (50–350 μm). The winding (vias, lines, and pads) made by silver or gold conductive pastes can be cofired with the magnetic ferrites at a temperature around 900 °C. The developed LTCC-based inductors and transformers are reliable, compatible with surface mount technology, and do not require hand winding.

More recently, LTCC-based ferrite materials have been studied to integrate into power electronics modules in order to reduce the size and cost of the modules [17]–[21]. The ferrites can be cofired with other dielectric and conductive materials to create hybrid power electronic circuits, or used as a substrate for attaching power semiconductor devices and other discrete components [17]. For instance, Roesler *et al*. reported the development of planar LTCC transformers for high-voltage flyback converters [18]; Wang *et al*. explored the design and fabrication of an ultrathin LTCC-based ferrite coupled inductor for dc/dc converters [19]; and Lim *et al.* demonstrated a low-profile ferrite inductor based on LTCC technology for power delivery applications [20], [21]. However, the integration technology of LTCC-based magnetic components with other functional parts is rarely reported in the literature.

A 3-D integration concept where the whole converter is assembled in a vertical fashion has been realized in this study. A low-profile passive layer is designed as a substrate for the whole converter and the active layer is mounted earlier. This vertical configuration allows a saving in footprint and a full space utilization, which greatly increases the power density of the converter. The key technologies in this integration solution can be summarized as low-profile magnetic component design and fabrication, high-frequency active layer design, and the integration of both passive and active layers. As mentioned earlier, the mixed low-temperature sintered ferrite laminate has shown desirable performance in the multimegahertz frequency range and is also applicable for integration with semiconductor devices. The following sections introduce the fabrication of a low-temperature sintered multilayer ferrite inductor substrate and its further integration with the active layer.

A. Preparation of Low-Temperature Sintered Multilayer Ferrite Inductors

A modified LTCC processing technique was used for the preparation of the planar low-profile ferrite inductors. A process diagram of the inductor fabrication is illustrated in Fig. 4. The ferrite tapes were first cut into 50 mm × 50 mm squares. A certain number of layers of the cut squares were then stacked alternatively one above another using two commercial low-temperature sinterable ferrite tapes, ESL 40010 and ESL 40012 (ElectroScience, King of Prussia, PA). Next, the stacked layers were placed between heated platens (70 °C) and pressed at 10 MPa for 15 min using a uniaxial hydraulic press (2112; Carver, Wabash, IN). The designed inductor geometry and conduction vias were cut out of the mixed ferrite laminates using a CO_2 laser system (Resonetics, Nashua, NH) after the lamination process. The additional vias were filled with silver paste (7740; DuPont Microcircuit Materials, Research Triangle Park, NC). Finally, ferrite laminates and compatible silver pastes were

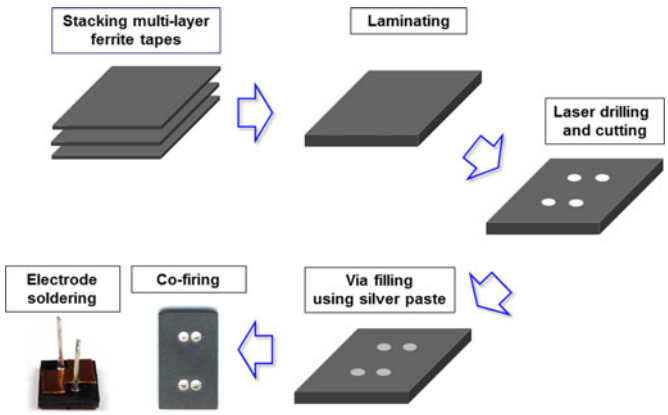

Fig. 4. Process flow of planar inductor fabrication using low-temperature sintered ferrite tapes and LTCC technology. The sintering shrinkages of 20% in the x–y direction and 15% in the z-direction for the mixed ferrite laminates have been taken into consideration in the design process. A prolonged sintering profile adjusted from the manufacturers' recommendation was determined in order to reduce stresses developed in the mixed ferrite laminates due to the different sintering behaviors of each type of layer. The silver paste was selected based on its higher conductivity than other similar products.

cofired at a peak temperature of 885 °C for 3.5 h on a flat porous zirconia setter in a box furnace (Vulcan 3-550; DENTSPLY International, York, PA) in air atmosphere. The organic binder was burnout at 450 °C for 1 h. Both temperature ramp-up and cool-down processes were controlled at the same rate of 0.5 °C/min. During the sintering process an additional pressure of 0.5 kPa was applied on top of the mixed ferrite laminates. After sintering, 0.3-mm-thick copper electrodes and two connection pins were soldered on the surface of the sintered inductors to generate the conductive winding for testing.

Laser machining of LTCC materials in the green (nonsintered) state has been widely used in industry, which allows fine-line patterning and reduces prototyping time and cost [22], [23]. Via drilling using a CO_2 laser system is a critical step in the fabrication of the LTCC-based multilayer ferrite inductors introduced in this study. Due to the thermal interaction between the laser beam and the ferrite laminates, material loss must be considered in the design process. The thickness of a single layer of ferrite tape is about 60 μm. It is necessary to laminate multiple layers to achieve the designed inductance. Laminating multilayer ferrite tapes first before laser drilling vias takes less prototype processing time than laminating the tapes after drilling the vias. However, the thickness of the laminate has a significant impact on the geometry of the drilled vias. The laser optical diffraction across the thickness can result in a nonvertical cutting wall, which may significantly lower the patterning resolution. A systematic study on the laser cutting loss and kerf taper of multilayer ferrite laminates demonstrates that the used CO_2 laser patterning technique has little effect on the thin laminates (layer numbers 2–14), while the thicker samples (layer numbers $>$14) are greatly affected by the laser-induced ablation zone. A laminate with an optimal number of layers ranging from 10 to 14 was determined as the building block for multilayer fabrication for a thick ferrite inductor.

B. Integration of Planar Inductors With Active Layers

The developed planar inductor substrate has to be connected with an active layer to realize the converter function. Direct bonded copper (DBC) and PCB are utilized for fabrication of the active layers. The DBC substrate provides better thermal performance, while the PCB substrate provides a cost-effective solution. The PCB substrate is used as an example in this section to demonstrate the integration process.

The LTCC process for inductor fabrication introduced in the previous section was slightly modified in order to facilitate further integration of the inductor substrate with the active layer. Ferrite laminates with laser drilled vias were first sintered alone in air. The patterned conductor vias were then filled with silver paste, but two of the vias at the diagonal corners were left blank. Filled silver paste was finally postfired on sintered ferrite laminates at 850 °C for 30 min. The copper electrodes were soldered on one side of the inductor substrate before bonding to the PCB active layer. The PCB-based active layers were manufactured based on the design, and all chips as well as passives were soldered on one side of the active layer. Two copper pins were then soldered on the other side of the active layer. The soldering sites were positioned to the empty holes that were left on the multilayer ferrite inductor. A solder mask was used to prevent excessive solder paste from spreading.

The selected thermal interface material (TIM) (SUPREME 10ANHT; MasterBond, Hackensack, NJ) in a paste form was applied evenly onto the active layer without components after soldering the pins and removing the solder mask. The inductor substrate was then attached with gentle pressure to the bonding layer. The inductor surface soldered with copper electrodes was in contact with the TIM. Subsequently, the TIM was cured at 120 °C for 90 min. A bonding layer, electrically nonconductive but thermally conductive, was firmly formed between the inductor substrate and the PCB active layer after curing. Finally, another set of copper electrodes were soldered on the exposed surface of the inductor substrate. An integrated POL with a low-temperature sintered ferrite inductor substrate and a PCB active layer was fabricated in this manner and used for further electrical testing and thermal reliability evaluation. A schematic drawing and photo images of an LTCC ferrite planar inductor and the assembled POL module working at 5 MHz are shown in Fig. 5.

Fig. 6 presents a microscopic image taken on the cut cross-section surface of an assembled module. No pores, cracks, or other major defects were observed on the cured TIM bonding layer, while, no delamination was found at the interfaces between the TIM and the copper on the PCB or the multilayer ferrite inductor. A fully assembled POL module is realized with all functional components integrated into one part. The limitations of this ceramic process include: sintering LTCC ferrite inductors around 900 °C, the cost of raw materials, and the difficult to achieve automatic production. The assembly approach introduced in the next section integrates a planar inductor using a traditional PCB manufacturing technique. This could intrigue industries whose target is a low-cost, mass-production available solution of manufacturing high power density POL converters.

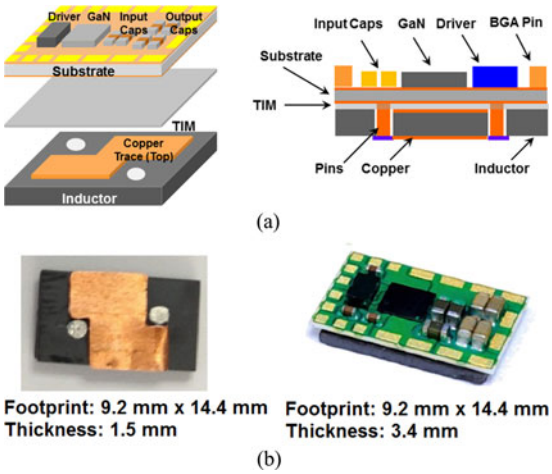

Fig. 5. (a) Structural drawing of integrated POL module. This structure includes three basic parts: the top active layer with a GaN transistor, a driver, connection pins, and input/output capacitors; the bottom ferrite inductor layer with copper electrodes; and the adhesive TIM layer in the middle. (b) Photos of LTCC ferrite planar inductor and assembled POL module working at 5 MHz with LTCC-based ferrite inductor substrate.

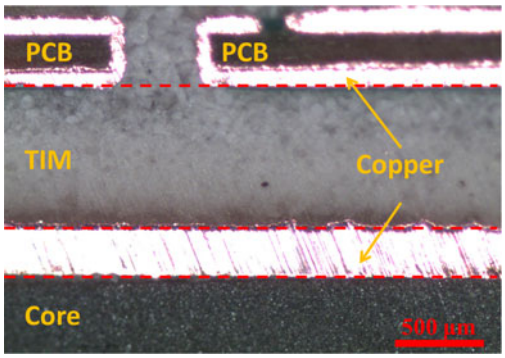

Fig. 6. Optical microscope image of the cross-sectional view of the assembled POL module with LTCC-based ferrite inductor substrate. The sample was mounted in epoxy and then cut using a diamond blade saw (VC-50; LECO, St. Joseph, MI) after epoxy curing. The exposed cross-sectional surface was ground and polished for observation. Other samples shown in this work for optical microscope or SEM observation were prepared using the same method.

IV. Processing of POL Modules With PCB-Embedded Metal-Flake Inductors

Embedding passive or active components into substrates (e.g., PCB and DBC) has gained interest from both academia and industry. The growing attention toward an embedded structure is not only because of the demand for higher power density but also the need for better electrical performance and reliability. Technologies for embedding passive components (e.g., inductors) into built-up layers of polymeric substrates have been investigated for more than a decade [24], [25]. Since most medium and high power converters use a PCB as the substrate, current research on embedding technology focuses on utilizing standard PCB materials and processes.

One promising magnetic material compatible with existing PCB processing is a ferrite polymer composite (FPC) that consists of ferrite powders dispersed in a polymer matrix. Such composite materials can be either laminated with PCB layers in sheet or tape format [26], [27], or directly deposited on the PCB by spin coating or screen printing [24], [28], [29]. Embedding FPC into the multilayer PCB saves the footprint of the magnetic components and removes the wasted space between the magnetics and the other components, thus, a higher power density can be achieved. Furthermore, the applied standard processes could reduce cost because it has fewer manual steps and no need for high temperatures. As an example, a 60 W resonant converter with PCB-integrated FPC magnetics as a transformer is reported in [26]. However, high core loss and the low permeability of FPC materials are problems for high-frequency operation.

Another approach of incorporating magnetic layers into PCB structures uses high permeability magnetic alloys, such as permalloys (Ni-Fe) [25], [30]–[32]. However, the thickness of this type of magnetic layer must be considerably thin to minimize the high-frequency eddy current loss because of its low resistivity. A PCB integrated flyback transformer for a 35 W power factor correction rectifier was demonstrated using tens of layers of stacked commercial alloy foils to realize only 0.66 mm core thickness. An electrical isolation layer was inserted between each magnetic layer [32]. The complex lamination process makes such alloy foils unsuitable for the high current level POL converters, where a large core volume is commonly needed. Some researchers have focused on embedding high-temperature sintered Mn-Zn ferrite cores (3F3 from Ferroxcube) with high permeability and low core loss density into the PCB as power inductors and transformers [33]. The drawback of this approach involves the laborious machining of rigid ferrite which requires costly high-precision milling equipment.

The fabrication of a prototype POL module with PCB-embedded metal-flake composite inductor has been introduced in this paper. A variety of magnetic anisotropic metal-flake composite materials have been developed and investigated for high-frequency applications, e.g., Fe-Si-Al alloy flake composites for electromagnetic interference (EMI) suppression [34], silica-coated Ni-Fe-Mo flake composites for high-frequency dc/dc converters [35] and EMI [36], and Ni-Fe composite materials for antennas [37]. The metallic magnetic materials with a saturation magnetization higher than that of ferrites are coated with insulating materials for the fabrication of the composites. Metallic particles are normally milled down to reduce the thickness to less than the skin depth, which is effective in decreasing the eddy current loss. As introduced in the magnetic characterization section, the metal-flake composite materials developed by NEC-TOKIN exhibit higher permeability and lower core loss density in the 1–3 MHz range than some sintered ferrites because of the alignment improvements and the volume ratio increment of magnetic flakes. Moreover, such composite materials are capable of being either molded as magnetic cores or built into thick-film format by tape casting. The thickness of the laminates can be built up to several millimeters. The laminated plate can be further processed by mechanical machining, and no high-temperature treatment is required. Thus, the NEC-TOKIN's metal-flake composite materials are ideal to realize PCB integration of the POL module with high output current, enabling cost-effective and automatic production processing.

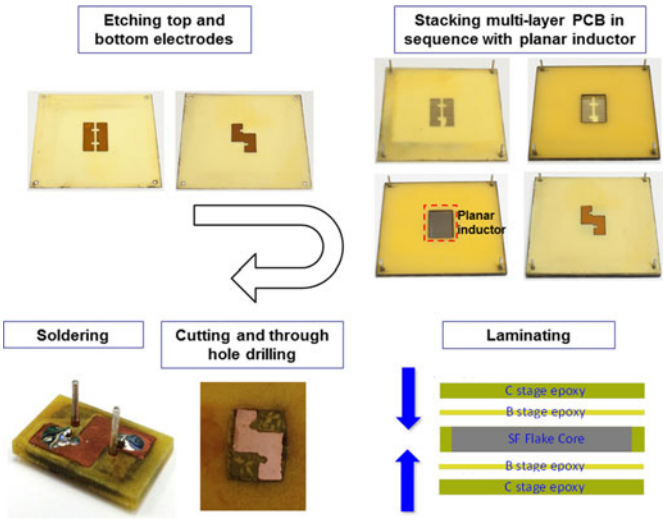

Fig. 7. Fabrication process of PCB-embedded planar inductor. The lamination parameters (pressure, temperature, and heating/cooling rates) need to be carefully controlled to avoid any damage to the embedding structure. A symmetric layout is recommended for a uniform pressure distribution in order to prevent severe warpage of the multilayer PCB substrate.

A. *Preparation of PCB-Embedded Inductor Substrate*

The commercial PCB materials used in this study, FR406 epoxy laminates and prepregs, were obtained from Isola. The process flow of fabricating a multilayer PCB structure with embedded metal-flake composite magnetic core is illustrated in Fig. 7. First, individual layers were prepared for building the multilayer PCB structure. The top and bottom layers were made of two C-stage fully cured copper cladded laminates. The surface winding on both layers were prepared by etching off extra copper using a bench-top etching machine (BTD-201B; Kepro Circuit Systems, St. Louis, MI). The middle layer was another C-stage laminate with an opening for inductor embedding. Two B-stage semicured prepregs were prepared as adhesive layers between the laminate layers. All of the layers were cut to the same dimensions. Alignment holes on the corners were laser drilled at every building layer, and a rectangular-shape cavity fit for the geometry of the embedded core was also formed in the middle layer. These cuts were made using the same CO_2 laser machine applied for cutting LTCC ferrite tapes. Then, the created layers were stacked in sequence with the assistance of alignment pins. The planar core made by NEC-TOKIN's metal-flake composite materials was embedded inside the multilayer PCB. Subsequently, the stack was laminated using a hydraulic press with heat and pressure profiles recommended by the manufacturer. The peak lamination temperature was 190 °C and the pressure applied was 2 MPa. The semicured epoxy in the prepregs was melted to adhere to different layers under specific temperatures and was fully cured after the lamination process. After lamination, the peripheral materials of the multilayer laminate were cut off, and four holes going through both the PCB layers and the magnetic core were drilled using a PCB milling machine (QC5000; T-Tech, Norcross, GA). Finally, the inductor winding was realized through pin soldering. Fig. 7 shows a two-turn planar inductor sandwiched into a two-layer PCB with a copper layer on the top and bottom. The low-profile inductor substrate with the lateral flux pattern can utilize the superiority of the metal-flake composite material, since the magnetic metal-flake is also laterally aligned.

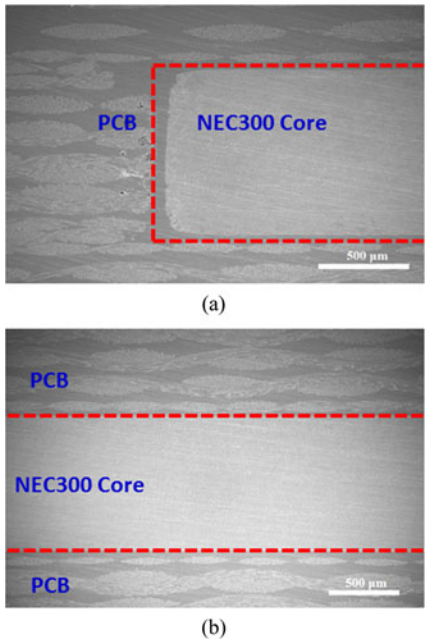

Fig. 8. SEM micrographs of laminated PCB substrate with embedded metal-flake composite inductor, (a) corner area and (b) middle area.

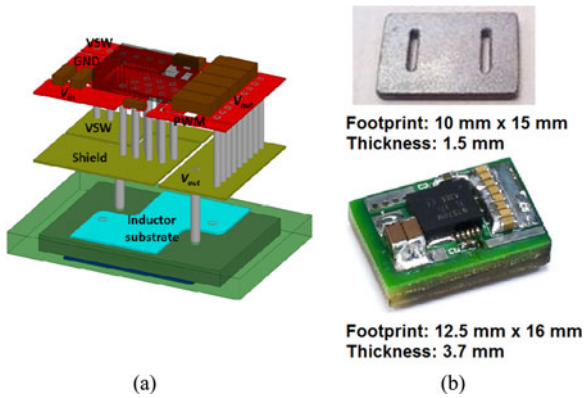

Fig. 9. (a) Diagram of an expanded view of the multilayer PCB structure with embedded planar inductor. (b) Photos of a planar inductor made of metal-flake composite material and a prototype of the integrated POL module working at 2 MHz with PCB-embedded inductor.

The PCB-embedded planar inductor was vertically sectioned to investigate the PCB lamination results. Fig. 8 shows the scanning electron microscope (SEM) image of a cross-sectional view of the multilayer PCB structure with the embedded core. The laminate was demonstrated to be cohesive by the lack of obvious cracking on both the PCB and core materials, and there was no delamination at their interfaces. As shown in Fig. 9(a), very few small pores were found on the PCB layers next to the vertical side of the core material, which was possibly due to volatiles that were generated during the lamination process and trapped afterwards. The application of a vacuum lamination technique would solve this problem.

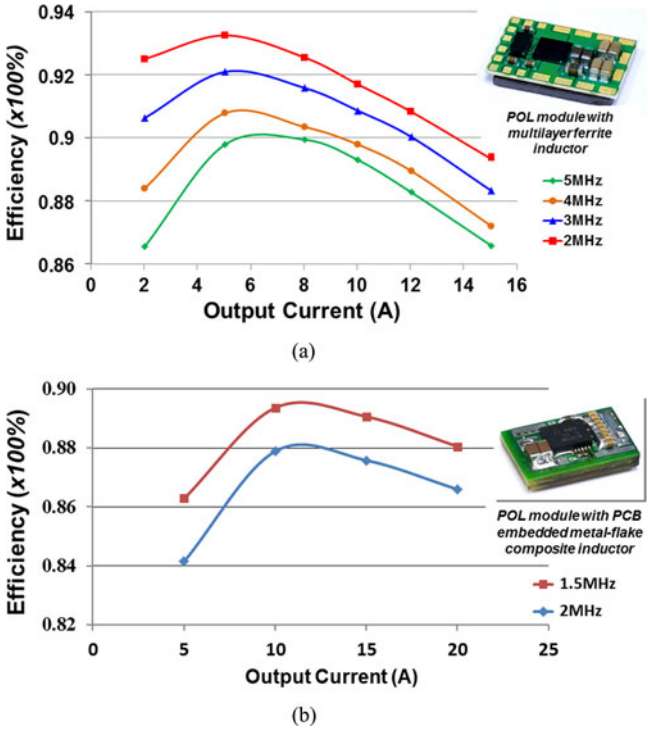

Fig. 10. Efficiency data of integrated 12 $V_{\rm in}$, 1.8 $V_{\rm out}$ single-phase POL modules with (a) ferrite inductor substrate and (b) PCB-embedded metal-flake composite inductor measured at different frequencies and output current levels.

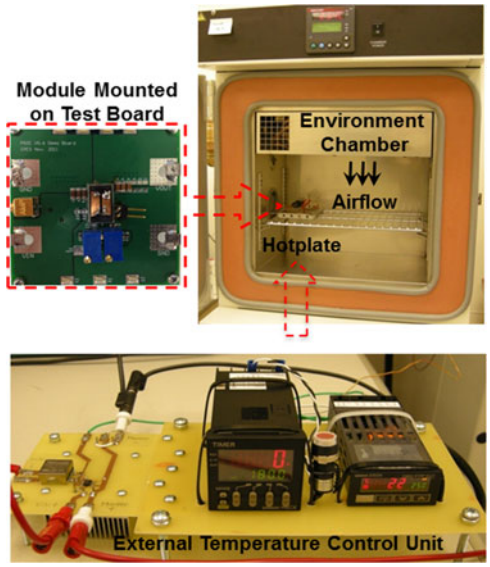

Fig. 11. Experimental setup of thermal cycling test. The testing module was placed on top of a hotplate which was used to heat up the sample inside the environmental chamber (Tenny TUJR; Thermal Product Solutions, White Deer, PA). The temperature of the chamber was constantly controlled at -40 °C for a sufficient cooling rate. During the experiment, the temperature ramp-up rate monitored on the testing module was carefully adjusted using an external control unit so as to create the required thermal profile.

B. Integration of PCB-Embedded Inductor Layer With Active Layers

The fabrication of an active layer was performed using the same PCB materials and designed active circuitry. Similar to LTCC-based integration techniques, two connection pins were soldered on the backside of the prepared active PCB layer. An additional lamination process was conducted to integrate a PCB-embedded core substrate with the top active layer. An additional prepreg layer was inserted in between the two parts. After lamination, the two connection pins through the PCB-embedded core were truncated to be flush with the bottom and soldered to the surface electrodes to generate a complete winding. All other components were finally surface-mounted on top of the active layer using one-step reflow soldering.

The designed magnetic layer becomes thinner when the operating frequency of the planar inductor is higher, which is beneficial because this increases the power density. From the core loss density data shown in Fig. 1, targeting the switching frequency of designed POL modules in the range of 1–2 MHz would be a reasonable choice. At this frequency range, the metal-flake composite material has a core loss that is comparable to or even lower than other high-frequency magnetic ferrites. On the other hand, silicon power devices rather than the GaN devices could be used to construct the POL modules, which would make this solution low-cost and easily adopted by industry. Therefore, working at 1–2 MHz is an acceptable tradeoff between power density and efficiency for a high current POL module built with silicon devices.

Fig. 9(a) illustrates the layout of this four-layer PCB-based module with embedded planar inductor. The laminated multilayer structure is expanded by intentionally enlarging the distance between each layer. All components except the inductor are placed on the top layer. The switching node point (VSW) and the output point $(V_{\rm out})$ at the top layer are connected to the pads on the second layer and to the lower surface winding of the inductor at the bottom layer through two conductive pins. The upper surface winding of the inductor at the third layer is connected to the lower surface winding at the bottom layer by two blind vias. The planar inductor is embedded between the third layer and the bottom layer. Part of the second layer acts as a shielding layer. The eddy current induced in the shielding layer creates an opposite flux to cancel the flux caused by the parasitic inductance of the high-frequency switching loop, which reduces the loop inductance and switching loss. A planar metal-flake inductor and the completely fabricated high-frequency POL module with PCB-embedded planar inductor are displayed in Fig. 9(b). The integrated module was used for further electrical and thermal characterizations.

V. Performance of High Power Density Integrated POL Modules

In order to maintain a desirable efficiency rating, the switching frequency of POLs is continuously decreased from the multimegahertz range to several hundreds of kilohertz, with an increasing current level. This is mainly because of the limitation of available power semiconductor devices and suitable magnetic materials. It is difficult to achieve both high efficiency and high frequency during operation of the POL converter with a high output current load.

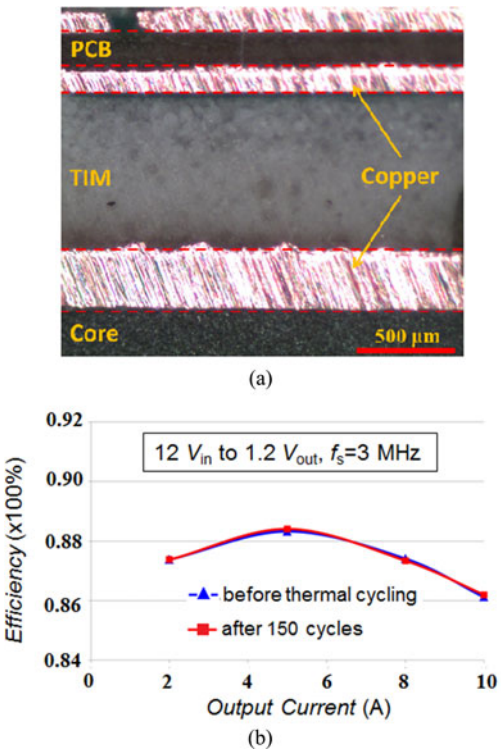

Fig. 12. (a) Optical microscopic observation of ferrite inductor integrated POL module after thermal reliability test. (b) Comparison of efficiency tested before and after thermal cycling. All efficiency data were measured at room atmosphere.

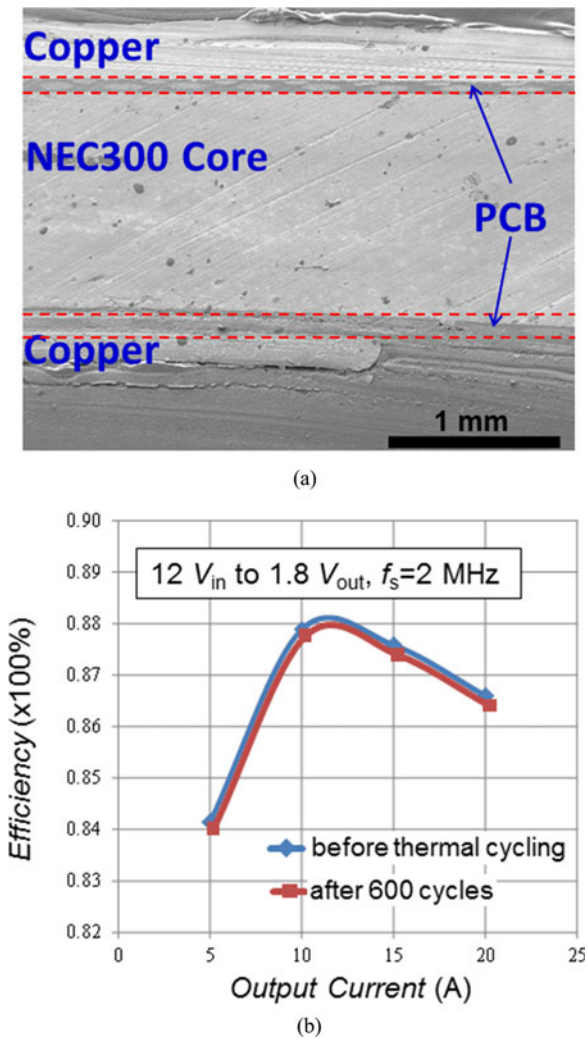

Fig. 13. (a) SEM image of POL module with PCB-embedded core after 600 thermal cycles. (b) Impact of thermal cycling test on the power module efficiency. All efficiency data were obtained at room atmosphere.

In our study, efficiencies were tested for a 12 $V_{\rm in}$ to 1.8 $V_{\rm out}$ conversion at different frequencies and load levels for both integrated POL modules. As illustrated in Fig. 10(a), the power efficiency measured at a high load level (15 A) for the POL module with low-temperature sintered ferrite inductor substrate can achieve 89% at 2 MHz and 87% at 5 MHz. At light load condition (5 A), the efficiency measured at 2 and 5 MHz increases to 93% and 90%, respectively. It can be seen from Fig. 10(b) that the POL module with the PCB-embedded core can achieve above 84% efficiency in the load current level ranging from 5 to 20 A and the peak efficiency is as high as 89% with an output current of 10 A at 1.5 MHz. For both modules tested at a 2 MHz operating frequency and 15 A output current, the efficiencies are over 87%, which is comparable to industry products with the same rating.

The package-level integrated POL modules developed in this study successfully demonstrate high power density converters operating at high frequencies and high current levels. The lateral-flux planar inductors were used as passive substrates while integrating active devices and the circuitry in a 3-D configuration. A POL module integrated with a high-frequency GaN device and the low-temperature sintered ferrite inductor substrate, working at 5 MHz and 15 A output current, achieves around 1000 W/in^3 power density. The other POL module fabricated using a silicon NexFET device developed by TI and a PCB-embedded metal-flake composite inductor obtains a power density of 800 W/in^3 at a high frequency (2 MHz) and a high current level (20 A). These two planar magnetic integrated modules can achieve five to eight times the power density with similar efficiency as the commercial modules at the same current level.

VI. Thermal Reliability Test

The thermal reliability of the fabricated hybrid power modules is a major concern in industry applications where significant stresses may occur at the interfaces between different materials due to the temperature swing. Such thermally induced stresses can result in defects, such as cracking and delamination, which eventually cause the module to fail. Therefore, it is important to examine the thermal withstand capability of the interconnects and the entire module.

A. Thermal Cycling Experimental Setup

Thermal cycling testing was used to assess the reliability of high-density integrated POL modules developed by both approaches. The temperature profile was determined according to the JEDEC standard JESD22-A104-D [38]. The temperature extremes were set at –40 and +150 °C. The cycle time was

45 min, and the dwelling time at each temperature extremes was 10 min. A customized experimental setup was applied in order to replicate the standard requirements, as shown in Fig. 11.

B. Testing Results

The POL module integrated with LTCC-based ferrite inductor was found after 150 thermal cycles to have no cracking, delamination, or other defects based on visual inspection using an optical microscope, as illustrated in Fig. 12(a). Although there was a large coefficient of thermal expansion mismatch among the different materials, the TIM bonding layer stayed securely attached to both the PCB active layer and inductor substrate layer without any signs of separation. In addition, the copper traces were not delaminated from the PCB and ferrite inductor substrates. It is also shown in Fig. 12(b) that the efficiency as measured before and after the thermal cycling test on this module are approximately the same. The fact that there was no performance degradation testifies to the reliability of all of the components and the developed integration technique.

As shown in the SEM image of the cross-sectional view in Fig. 13(a), no delamination was observed on any of the heterogenous interfaces in the module with the PCB-embedded inductor after 600 thermal cycles. Only a slight bending was found on the bottom PCB layer where no copper trace was attached. Additionally, very few small pores and cracks were examined in the metal-flake composite material embedded within the multilayer PCB. However, the efficiency of the module has a negligible change after thermal cycling, as shown in Fig. 13(b). This validates the thermal reliability of this integrated module with a multilayer PCB-embedded magnetic core.

VII. Conclusion

The bulky conventional discrete magnetic component is a bottleneck for high-frequency high-current power conversion in a high-density format. In this study, the planar inductors that worked as passive substrates were prepared and integrated into the POL modules in order to improve the power density. Two approaches were used: 1) hybrid integration of the LTCC-based ferrite inductor substrate with a PCB active layer and 2) embedding planar magnetic core in a PCB multilayer structure using associated technology. The integrated POL modules, as demonstrated by prototypes, can achieve more than 87% efficiency at a high frequency (2 MHz) and a high output current level (15 A). The determined power densities of a 15 A, 5 MHz POL module integrated with ferrite inductor substrate and a 20 A, 2 MHz module assembled using a PCB-embedded inductor are 1000 W/in^3 and 800 W/in^3, respectively. Both assembled POL modules survive after hundreds of thermal cycles, validating the reliability of all integrated components and the compatibility of magnetic materials with traditional PCB materials. Additionally, fabrication of PCB-embedded inductor POL modules using standard PCB technology, in contrast to making modules with multilayer ferrite inductors, may reduce manufacturing cost due to the possible mass-production and relatively low processing temperature.

The developed assembly technologies overcome the challenges of integrating high power density POL modules and enable high-frequency high-current applications, which satisfy the continuous demand for miniaturization of POL modules. The basic fabrication techniques used in this study, such as LTCC processing, PCB lamination, and device surface mounting, are directly adapted from industrial standard processes and are compatible with real manufacturing production. Therefore, the successful demonstration of these fabricated high power density high efficiency POL modules may excite tremendous interest from industry. Still, the prospective power density of integrated POL converters could be pushed to an even higher level, with the development of semiconductors, magnetics, inductor and circuit designs, and integration technology. Continuous efforts will be made to deliver high efficiency power at an ever-increasing need for high power density.

Acknowledgment

The authors would like to thank Dr. D. Hou for his assistance in the magnetic property measurements. They would also like to thank Dr. Z. Chen for his help on the thermal experimental setup. A special thanks also to Isola for supporting PCB materials and CPES industry member NEC-TOKIN, who provided metal-flake composite materials used in this paper.

References

[1] C. O. Mathuna, P. Byrne, G. Duffy, W. Chen, M. Ludwig, T. O'Donnell, P. McCloskey, and M. Duffy, "Packaging and integration technologies for future high-frequency power supplies," *IEEE Trans. Ind. Electron.*, vol. 51, no. 6, pp. 1305–1312, Dec. 2004.

[2] F. C. Lee and Q. Li, "High-frequency integrated point-of-load converters: Overview," *IEEE Trans. Power Electron.*, vol. 28, no. 9, pp. 4127–4136, Sep. 2013.

[3] C. O. Mathuna, N. Wang, S. Kulkarni, and S. Roy, "Review of integrated magnetics for power supply on chip (PwrSoC)," *IEEE Trans. Power Electron.*, vol. 27, no. 11, pp. 4799–4816, Nov. 2012.

[4] C. R. Sullivan, D. V. Harburg, J. Qiu, C. G. Levey, and D. Yao, "Integrating magnetics for on-chip power: A perspective," *IEEE Trans. Power Electron.*, vol. 28, no. 9, pp. 4342–4353, Sep. 2013.

[5] Y. Su, Q. Li, M. Mu, and F. C. Lee, "High frequency inductor design and comparison for high efficiency high density POLs with GaN device," in *Proc. Energy Conv. Cong. Expo.*, 2011, pp. 2146–2152.

[6] Y. Su, Q. Li, M. Mu, D. Gilham, D. Reusch, and F. C. Lee, "Low profile LTCC inductor substrate for multi-MHz integrated POL converter," in *Proc. IEEE Appl. Power Electron. Conf. Expo.*, 2012, pp. 1331–1337.

[7] D. Reusch, F. C. Lee, D. Gilham, and Y. Su, "Optimization of a high density gallium nitride based non-isolated point of load module," in *Proc. Energy Conv. Cong. Expo.*, 2012, pp. 2914–2920.

[8] S. Ji, D. Reusch, and F. C. Lee, "High-frequency high power density 3-D integrated gallium-nitride-based point of load module design," *IEEE Trans. Power Electron.*, vol. 28, no. 9, pp. 4216–4226, Sep. 2013.

[9] Y. Su, W. Zhang, Q. Li, F. C. Lee, and M. Mu, "High frequency integrated point of load (POL) module with PCB embedded inductor substrate," in *Proc. Energy Conv. Cong. Expo.*, 2013, pp. 1243–1250.

[10] M. Mu, Q. Li, D. Gilham, F. C. Lee, and K. D. T. Ngo, "New core loss measurement method for high frequency magnetic materials," in *Proc. Energy Conv. Cong. Expo.*, 2010, pp. 4383–4389.

[11] M. Mu, F. C. Lee, Q. Li, D. Gilham, and K. D. T. Ngo, "A high frequency core loss measurement method for arbitrary excitations," in *Proc. IEEE Appl. Power Electron. Conf. Expo.*, 2010, pp. 157–162.

[12] M Mu, Y. Su, Q. Li, and F. C. Lee, "Magnetic characterization of low temperature co-fired ceramic (LTCC) ferrite materials for high frequency power converters," in *Proc. Energy Conv. Cong. Expo.*, 2011, pp. 2133–2138.

[13] W. Zhang, M. Mu, D. Hou, Y. Su, Q. Li, and F. C. Lee, "Characterization of low temperature sintered ferrite laminates for high frequency point-of-load (POL) converters," *IEEE Trans. Magn.*, vol. 49, no. 11, pp. 5454–5463, Nov. 2013.
[14] G. Slama, "Low-temperature co-fired magnetic tape yields high benefits," *Power Electron. Technol.*, vol. 29, no. 1, pp. 30–34, Jan. 2003.
[15] R. L. Wahlers, C. Y. D. Huang, M. R. Heinz, A. H. Feingold, J. Bielawski, and G. Slama, "Low profile LTCC transformers," in *Proc. SPIE Int. Soc. Opt. Eng.*, 2002, pp. 76–80.
[16] R. Hahn, S. Krumbholz, and H. Reichl, "Low profile power inductors based on ferromagnetic LTCC technology," in *Proc. Electron. Comp. Technol. Conf.*, 2006, pp. 517–523.
[17] W. Roesler, J. M. Schare, C. Hettler, D. Abel, G. Slama, and D. Schofield, "Integrated power electronics using a ferrite-based low-temperature co-fired ceramic materials system," in *Proc. Electron. Comp. Technol. Conf.*, 2010, pp. 720–726.
[18] W. Roesler, J. M. Schare, S. J. Glass, K. G. Ewsuk, G. Slama, D. Abel, and D. Schofield, "Planar LTCC transformers for high-voltage flyback converters," *IEEE Trans. Compon. Packag. Technol.*, vol. 33, no. 2, pp. 359–372, Jun. 2010.
[19] L. Wang, Y. Pei, X. Yang, and Z. Wang, "Design of ultrathin LTCC coupled inductors for compact DC/DC converters," *IEEE Trans. Power Electron.*, vol. 26, no. 9, pp. 2528–2541, Sep. 2011.
[20] M. H. Lim, Z. Liang, and J. D. van Wyk, "Low profile integratable inductor fabricated based on LTCC technology for microprocessor power delivery applications," *IEEE Trans. Compon. Packag. Technol.*, vol. 30, no. 1, pp. 170–177, Mar. 2007.
[21] M. H. Lim, J. D. van Wyk, F. C. Lee, and K. D. T. Ngo, "A class of ceramic-based chip inductors for hybrid integration in power supplies," *IEEE Trans. Power Electron.*, vol. 23, no. 3, pp. 1556–1563, Mar. 2008.
[22] J. Kita, A. Dziedzic, L. J. Golonka, and T. Zawada, "Laser treatment of LTCC for 3D structures and elements fabrication," *Microelectron. Int.*, vol. 19, no. 3, pp. 14–18, 2002.
[23] K. M. Nowak, H. J. Baker, and D. R. Hall, "Cold processing of green state LTCC with a CO_2 laser," *Appl. Phys. A: Mater. Sci. Process.*, vol. 84, pp. 267–270, 2006.
[24] J. Y. Park and M. G. Allen, "Low temperature fabrication and characterization of integrated packaging–compatible, ferrite-core magnetic devices," in *Proc. IEEE Appl. Power Electron. Conf. Expo.*, 1997, pp. 361–367.
[25] Y. Zhang and S. Sanders, "In-board magnetics processes," in *Proc. IEEE Power Electron. Special. Conf.*, 1999, pp. 562–567.
[26] E. Waffenschmidt, B. Ackermann, and J. A. Ferreira, "Design method and material technologies for passives in printed circuit board embedded circuits," *IEEE Trans. Power Electron.*, vol. 20, no. 3, pp. 576–584, May 2005.
[27] E. Waffenschmidt and J. A. Ferreira, "Embedded passives integrated circuits for power converters," in *Proc. Power Electron. Special. Conf.*, 2002, pp. 12–17.
[28] D. H. Bang and J. Y. Park, "Ni-Zn ferrite screen printed power inductors for compact DC-DC power converter applications," *IEEE Trans. Magn.*, vol. 45, no. 6, pp. 2762–2765, Jun. 2009.
[29] D. Dening, S. Dorn, M. Shah, Y. Rao, M. Kay, and J. Jorgenson, "Circuit board embedded inductor," U.S. Patent 7 474 189 B1, Jan. 6, 2009.
[30] S. O'Reilly, M. Duffy, T. O'Donnell, P. McCloskey, C. O. Mathuna, M. Scott, and N. Young, "New integrated planar magnetic cores for inductors and transformers fabricated in MCM-L technology," *J. Microelectron. Electron. Packag.*, vol. 23, no. 1, pp. 62–69, Jan.–Mar. 2000.
[31] M. Ludwig, M. Duffy, T. O'Donnell, P. McCloskey, and C. O. Mathuna, "PCB integrated inductors for low power DC/DC converter," *IEEE Trans. Power Electron.*, vol. 18, no. 4, pp. 937–945, Jul. 2003.
[32] C. Marxgut, J. Muhlethaler, F. Krismer, and J. W. Kolar, "Multi-objective optimization of ultra-flat magnetic components with a PCB-integrated core," in *Proc. IEEE Inter. Conf. on Power Electron. ECCE Asia*, 2011, pp. 460–467.
[33] Q. Chen, Z. Gong, X. Yang, and Z. Wang, "Design consideration for passive substrate with ferrite materials embedded in printed circuit board," in *Proc. Power Electron. Special. Conf.*, 2007, pp. 1043–1047.
[34] S. Yoshida, M. Sato, E. Sugawara, and Y. Shimada, "Permeability and electromagnetic-interference characteristics of Fe-Si-Al alloy flakes-polymer composite," *J. Appl. Phys.*, vol. 85, no. 8, pp. 4636–4638, 1999.
[35] Y. Zhou, X. Kou, M. Mu, B. M. McLaughlin, X. Chen, P. E. Parsons, H. Zhu, A. Ji, F. C. Lee, and J. Q. Xiao, "Loss characterization of Mo-doped FeNi flake for DC-to-DC converter and MHz frequency applications," *J. Appl. Phys.*, vol. 111, pp. 07E329-01–07E329-03, 2012.
[36] Z. Raolison, C. Lefevre, J. Neige, A. L. Adenot-Engelvin, G. Pourroy, and N. Vukadinovic, "Preparation and microwave properties of silica coated Ni-Fe-Mo flakes composites," *IEEE Trans. Magn.*, vol. 49, no. 3, pp. 986–989, Mar. 2013.
[37] Y. Shirakata, N. Hidaka, M. Ishitsuka, A. Teramoto, and T. Ohmi, "High permeability and low loss Ni-Fe composite material for high frequency applications," *IEEE Trans. Magn.*, vol. 44, no. 9, pp. 2100–2106, Sep. 2008.
[38] Temperature Cycling, JEDEC Standard No. 22-A104D, 2009.

Wenli Zhang received the B.S. and M.S. degrees in materials science and engineering from Beijing University of Technology, China, in 2003 and 2006, respectively, and the Ph.D. degree from the University of Kentucky, Lexington, in 2011, in the area of advanced ceramic materials and processing.

He is currently a Research Assistant Professor working in the Center for Power Electronics Systems at Virginia Polytechnic Institute and State University. His research interests include piezoelectric and magnetic ceramics, LTCC materials and technology, high density integration of power electronics modules.

Dr. Zhang is a member of the MRS, the ACerS, and the IMAPS.

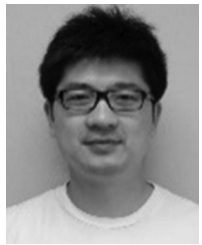

Yipeng Su (S'07) received the B.S. degree in electrical engineering from Tsinghua University, Beijing, China, in 2005, and the M.Phil. degree from the City University of Hong Kong, Kowloon, China, in 2008. He is currently working toward the Ph.D. degree in the Center for Power Electronics Systems, Virginia Polytechnic Institute and State University, Blacksburg, VA, USA.

From September to December 2008, he was as a Research Associate at the Center for Power Electronics, City University of Hong Kong. His main research interests include low-profile magnetic design, circuit integration in power electronics, and high-frequency power conversion.

Mingkai Mu received the B.S. and M.S. degrees in electronics engineering from Zhejiang University, China, in 2004 and 2007, respectively, and the Ph.D. degree from Virginia Polytechnic Institute and State University, Blacksburg, VA, USA, in 2013.

He is currently working as a Research Scientist at Center for Power Electronics Systems, Virginia Polytechnic Institute and State University. His research interests include high-frequency magnetics, high-power density integration, and high frequency power conversion.

David J. Gilham received the B.S and M.S. degrees in electrical engineering from Virginia Polytechnic Institute and State University, Blacksburg, VA, USA, in 2007 and 2013, respectively.

Since 2007, he has been with the Center for Power Electronic Systems, where he is currently the Electrical Lab Manager and Research Associate. His research interests include high-frequency converters, magnetic materials, and hybrid packaging using ceramic substrates.

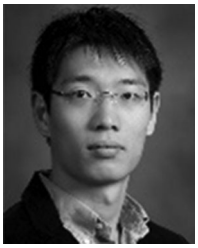

Qiang Li (M'12) received the B.S. and M.S. degrees in power electronics from Zhejiang University, China, in 2003 and 2006, respectively, and the Ph.D. degree from Virginia Polytechnic Institute and State University, Blacksburg, VA, USA, in 2011.

He is currently an Assistant Professor in the Center for Power Electronics Systems, Virginia Polytechnic Institute and State University. His research interests include high-density electronics packaging and integration, high-frequency magnetic components, and high-frequency power conversion.

Fred C. Lee (S'72–M'74–SM'87–F'90–LF'12) received the B.S. degree from the National Cheng Kung University, Tainan, Taiwan, in 1968, and the M.S. and Ph.D. degrees from Duke University, Durham, NC, USA, in 1972 and 1974, respectively, all in electrical engineering.

He is currently a University Distinguished Professor at Virginia Polytechnic Institute and State University, Blacksburg, VA, USA, where he is also the Director of the Center for Power Electronics Systems (CPES), a National Science Foundation Engineering Research Center (NSF ERC) established in 1998. Over the ten-year NSF ERC Program, CPES has been cited as a model ERC for its industrial collaboration and technology transfer, as well as education and outreach programs. He holds 75 U.S. patents and has published over 270 journal articles and more than 660 refereed technical papers. During his tenure at Virginia Tech, he has supervised to completion 76 Ph.D. and 83 Master's students. His research interests include high-frequency power conversion, distributed power systems, renewable energy, power quality, high-density electronics packaging and integration, and modeling and control.

Dr. Lee received the William E. Newell Power Electronics Award in 1989, the Arthur E. Fury Award for Leadership and Innovation in Advancing Power Electronic Systems Technology in 1998, and the Ernst-Blickle Award for achievement in the field of power electronics in 2005. He has served as president of the IEEE Power Electronics Society during 1993–1994. He was named to the National Academy of Engineering in 2011. In 2012, he was elected to Academia Sinica in Taiwan and inducted into Virginia Tech Faculty Entrepreneur Hall of Fame. He is also a foreign member of the Chinese Academy of Engineering in People's Republic of China.